
Neural Bregman Divergences for Distance Learning

Fred Lu

Booz Allen Hamilton

University of Maryland, Baltimore County

lu_fred@bah.com

Edward Raff

Booz Allen Hamilton

University of Maryland, Baltimore County

raff_edward@bah.com

Francis Ferraro

University of Maryland, Baltimore County

ferraro@umbc.edu

Abstract

Many metric learning tasks, such as triplet learning, nearest neighbor retrieval, and visualization, are treated primarily as embedding tasks where the ultimate metric is some variant of the Euclidean distance (e.g., cosine or Mahalanobis), and the algorithm must learn to embed points into the pre-chosen space. The study of non-Euclidean geometries or appropriateness is often not explored, which we believe is due to a lack of tools for learning non-Euclidean measures of distance. Under the belief that the use of asymmetric methods in particular have lacked sufficient study, we propose a new approach to learning arbitrary Bregman divergences in a differentiable manner via input convex neural networks. Over a set of both new and previously studied tasks, including asymmetric regression, ranking, and clustering, we demonstrate that our method more faithfully learns divergences than prior Bregman learning approaches. In doing so we obtain the first method for learning neural Bregman divergences and with it inherit the many nice mathematical properties of Bregman divergences, providing the foundation and tooling for better developing and studying asymmetric distance learning.

1 Introduction

Learning a task-relevant metric among samples is a common application of machine learning, with use in retrieval, clustering, and ranking. A classic example of retrieval is in visual recognition where, given an object image, the system tries to identify the class based on an existing labeled dataset. To do this, the model can learn a measure of similarity between pairs of images, assigning small distances between images of the same object type. Given the broad successes of deep learning, there has been a recent surge of interest in deep metric learning—using neural networks to automatically learn these similarities [1–3].

The traditional approach to deep metric learning learns an embedding function over the input space so that a simple distance measure between pairs of embeddings corresponds to task-relevant spatial relations between the inputs. The embedding function f is computed by a neural network, which is learned to encode those spatial relations. For example, we can use the basic Euclidean distance metric to measure the distance between two samples x and y as $\|f(x) - f(y)\|_2$. This distance is critical in two ways. First, it is used to define the loss functions, such as triplet or contrastive loss, to dictate *how* this distance should be used to capture task-relevant properties of the input space. Second, since f is trained to optimize the loss function, the distance influences the embedding function that is learned.¹

¹Outside of deep learning, the classic approach to metric learning aims to fit a Mahalanobis distance, represented as $\|W(x - y)\|_2$. This can be viewed as a special case where the embedding is a linear layer.

This approach has limitations. When the underlying reference distance is asymmetric or does not follow the triangle inequality, a standard metric cannot accurately capture the data. An important example is clustering over probability distributions, where the standard k-means approach with Euclidean distance is sub-optimal, leading to alternatives like the KL-divergence [4]. Other cases include textual entailment and learning graph distances which disobey the triangle inequality.

Can we generalize the distance measure in a manner that can be learned? A natural class of distances that include common measures such as the squared Euclidean distance are the Bregman divergences [5]. They are parametrized by a strictly convex function and measure the distance between two points x and y as the first-order Taylor approximation error of the function originating from y at x . The goal is that by learning a Bregman divergence we can infer an appropriate metric from data, instead of fixing the Euclidean distance as the final metric between embeddings.

In this work we describe Neural Bregman Divergences (NBD). Our core contributions are: 1) we present a novel approach to accurately learn Bregman measures using input convex neural networks (§2); 2) we show that our method is superior on existing Bregman divergence tasks, including regression, ranking, and clustering (§4); 3) we further study the performance of our method on asymmetric tasks where the underlying metric is not known to be Bregman. Our method performs reasonably on such tasks (§5). We also show that the previous deep divergence learning approach fails to learn effectively on many tasks. We thus obtain the first successful method for learning neural Bregman divergences, providing foundation and tooling for better developing and studying asymmetric distance learning.

2 Neural Bregman divergence learning

A Bregman divergence computes the divergence between two points x and y that live in a space \mathcal{X} by taking first-order Taylor approximations of a generating function ϕ . This generating function is defined over \mathcal{X} and can be thought of as (re-)encoding points from \mathcal{X} . A proper and informative ϕ is incredibly important: different ϕ can capture different properties of the spaces over which they are defined. Our aim in this paper is to learn Bregman divergences by providing a neural method for learning informative functions ϕ .

More formally, let $x, y \in \mathcal{X}$, where $\mathcal{X} \subseteq \mathbb{R}^d$. The generating function ϕ must be a continuously differentiable, strictly convex $\phi : \mathcal{X} \rightarrow \mathbb{R}$. We refer to the **Bregman divergence** parametrized by ϕ as $D_\phi(x, y)$, defined as:

$$D_\phi(x, y) = \phi(x) - \phi(y) - \langle \nabla \phi(y), x - y \rangle, \quad (1)$$

where $\langle \cdot, \cdot \rangle$ represents the dot product and $\nabla \phi(y)$ is the gradient of ϕ evaluated at y . For example, if $\mathcal{X} = \mathbb{R}^d$ and ϕ is the squared L_2 norm ($\phi(y) = \|y\|_2^2$), then $\nabla \phi(y) = 2y$. This yields the divergence $D_\phi(x, y) = \|x - y\|_2^2$.

A properly defined ϕ can capture critical, inherent properties of the underlying space. By learning ϕ via Eq. (1), we aim to automatically learn these properties. For example, Bregman divergences can capture asymmetrical relations: if \mathcal{X} is the D -dimensional simplex representing D -dimensional discrete probability distributions then $\phi(x) = \langle x, \log x \rangle$ yields the KL divergence, $D_\phi(x, y) = \sum_d x_d \log \frac{x_d}{y_d}$. Perhaps surprisingly, as we show in this paper, the central requirement of a Bregman divergence—that ϕ is strictly convex and continuously differentiable—is not a big limitation.

Focusing on the hypothesis space of Bregman divergences is valuable due to the fact that many core machine learning measures are special cases of Bregman divergences. This includes the squared Euclidean, Kullback-Leibler, and Ikura-Saito divergences. While special cases of the Bregman divergence are used today, and many general results have been proven over the space of Bregman measures, less progress has been made in *learning* Bregman divergences.

Prior works [6, 7] have examined max-affine representations of ϕ for mathematical convenience, as it allows the right hand side of Eq. (1) to cancel out and to directly work with the representation $D_\phi(x, y)$. By showing that their representation results in a valid $D_\phi(x, y)$ under correct constraints they are able to apply their learning approach to maintain those constraints. However, this comes at significant cost to run-time and representational capacity [6, 7]. Furthermore a max-affine representation, being piecewise linear, does not yield a smooth (continuously differentiable) divergence. Instead, we advocate for learning the convex function ϕ directly, as we describe below.

2.1 Representing D_ϕ via ϕ directly

To obtain an appropriate convex function ϕ to represent D_ϕ , we must resolve two constraints: 1) how to compute D_ϕ from just ϕ in an efficient manner; and 2) how to learn ϕ itself and guarantee that it is convex. We find that with some strategic design choices both of these constraints can be satisfied easily in a fully differentiable manner over the input space. This essentially reduces to learning the best ϕ among the class of strictly convex functions.

Efficient Computation. The first constraint of efficient computation can be tackled using a technique known as double backpropagation [8] to compute the $\nabla\phi(y)$ term. Normally computing the gradient of $\nabla\phi(y)$ would involve constructing the Hessian, with a resulting quadratic increase in computation and memory use. Double backpropagation allows us to use automatic differentiation to efficiently compute gradients with respect to the inputs in an efficient manner, and the dot-product between a gradient and another value in particular has specialized “Jacobian vector product” [9] operation that ensures $\langle \nabla\phi(y), x - y \rangle$ can be computed in the cost of evaluating $\phi(y)$ one additional time. Since there are already three calls to ϕ , this is only a 25% increase in computational overhead to backpropagate through Eq. (1), provided we have a learnable representation of ϕ . This functionality has been implemented in PyTorch in the `torch.autograd.functional` API [10].

Convexity of ϕ . To represent ϕ , we adopt the Input Convex Neural Network (ICNN) developed by Amos et al. [11]. The ICNN composes linear layers with non-negative weights W^+ and affine functions with unconstrained weights U with convex activation functions $g(\cdot)$. The composition of these three components for the i th layer of an ICNN is given by Eq. (2), with z_i the i th layer’s input and z_{i+1} the output,

$$z_{i+1} = g(W_i^+ z_i + U_i z_0 + b_i). \quad (2)$$

By construction, the resulting neural network satisfies convexity. Chen et al. [12] and Pitis et al. [13] have shown under specific conditions that ICNNs universally approximate convex functions.

Prior works on the ICNN have only tried piecewise linear activation functions such as the ReLU variants for $g(\cdot) = \max(x, 0)$; we instead use the Softplus activation $g(x) = \log(1 + \exp(x))$ which lends the network smoothness and strict convexity. This is an important design choice as evaluating $\nabla\phi(y)$ involves the second derivatives, which for any piecewise learning activation is zero almost everywhere. This causes vanishing gradients in the computation of $\langle \nabla\phi(y), x - y \rangle$ and restricts its capacity to learn. In our tests ReLU activation functions prevented effective learning entirely. Thus our choice of $g(x)$, combined with an appropriate parametrization of the non-negative layers in the ICNN, outperforms the default approach in divergence learning tasks.

2.2 Joint Training

The original feature space is rarely ideal for computing the distance measures between samples. Classical metric learning generally attempts to apply a linear transformation to the feature space in order to apply a fixed distance function $D(\cdot, \cdot)$ such as Euclidean distance [14, 15]. In deep metric learning, a neural network f_θ is used to embed the samples into a latent space where the distance function is more useful [16]. In our approach, instead of fixing the distance function, we also learn a Bregman divergence as the measure:

$$\begin{aligned} D_\phi(f_\theta(x), f_\theta(y)) = & \\ & \phi(f_\theta(x)) - \phi(f_\theta(y)) - \\ & \langle \nabla\phi(\tilde{y}), f_\theta(x) - f_\theta(y) \rangle \end{aligned} \quad (3)$$

with \tilde{y} evaluated as $f_\theta(y)$.

Note we now have two sets of parameters to learn: those associated with ϕ and those associated with the encoder (θ). During training,

Algorithm 1 Neural Bregman Divergence (NBD) Learning. Given data tuples (a_i, b_i) , our approach (1) learns f_θ to compute effective ways of featurizing a_i and b_i ; and (2) learns a function ϕ that can be used to compute a Bregman divergence value \hat{y} between the featurized data points. The computed Bregman divergence is trained via a task-specific loss function ℓ to be close to a *target* divergence value y_i . If a target divergence value isn’t available, an implicit loss function can be used.

Require: Dataset of pairs and target distance, Loss function $\ell(\cdot, \cdot) : \mathbb{R} \rightarrow \mathbb{R}$

- 1: $f_\theta \leftarrow$ any arbitrary neural network as a feature extractor
- 2: $\phi \leftarrow$ a ICNN network parameterized as by Eq. (2)
- 3: **for** each data tuple (a_i, b_i) with label y_i in dataset **do**
- 4: $\mathbf{x} \leftarrow f_\theta(a_i)$ ▷ Perform feature extraction
- 5: $\mathbf{y} \leftarrow f_\theta(b_i)$
- 6: $rhs \leftarrow \langle \nabla\phi(\mathbf{y}), \mathbf{x} - \mathbf{y} \rangle$ ▷ Using double backprop
- 7: $\hat{y} \leftarrow \phi(\mathbf{x}) - \phi(\mathbf{y}) - rhs$ ▷ Empirical Bregman
- 8: $\ell(\hat{y}, y_i).backward()$ ▷ Compute gradients
- 9: update parameters of ϕ and θ
- 10: **return** Jointly trained feature extractor f_θ and learned Bregman Divergence ϕ

and those associated with the encoder (θ). During training,

they are simultaneously learned through gradient descent, which involves back-propagating through the gradient function $\nabla\phi(\cdot)$ to update θ via double backpropagation [8]. We summarize this process in Alg. 1. The metric model accepts two samples as input and estimates the divergence between them. If and when the target divergence value is available, the metric can be trained using a regression loss function such as mean square error. Otherwise, an implicit comparison such as triplet or contrastive loss can be used.

3 Comparison to related work

In classic metric learning methods, a linear or kernel transform on the ambient feature space is used, combined with a standard distance function such as Euclidean or cosine distance. The linear case is equivalent to Mahalanobis distance learning. Information on and examples of such approaches include [17, 15, 14, 18]. Bregman divergences generalize many standard distance measures and can further introduce useful properties such as asymmetry. They have classically been used in machine learning for clustering, by modifying the distance metric used in common algorithms such as kmeans [4, 19].

One of the first methods to learn a Bregman divergence fits a non-parametric kernel to give a local Mahalanobis metric. The coefficients for the data points are fitted using subgradient descent [19]. More recently, Siahkamari et al. [7] directly learns a Bregman divergence by approximating the convex function ϕ using piecewise affine functions. This is formulated and solved as a convex optimization problem [7]. While theoretical approximation error bounds are available in this setting, such approaches do not scale well for large datasets and non-convex optimization scenarios typical for deep learning. We include this benchmark, denoted *PBDL*, in our ranking and clustering tasks.

Along the same vein as *PBDL*, Cilingir et al. [6] aims to learn a deep Bregman divergence using a neural network embedding followed by a separate dense subnetworks that represent piecewise affine functions. Because the convex function ϕ is approximated from below by affine functions, the tangent to input y is equivalent to the affine function at $\phi(y)$, denoted as f_y . Letting $f_x(x)$ represent the value at point x , this simplifies the Bregman divergence $D(x, y)$ as $f_x(x) - f_y(x)$. The network, consisting of the embedding layers and the affine subnetworks, are trained using gradient descent. We include this method, denoted *Deep-div*, as our primary Bregman benchmark. While the method performs reasonably on Bregman ranking and clustering tasks, we observe issues when training the network as described in their paper for more complex tasks such as deep metric learning or regression. Our method directly learns a continuous input convex neural network as ϕ rather than a piecewise approximation, and in doing so converges consistently to lower error solutions.

Pitis et al. [13] approach asymmetric distance learning by fitting a norm N with modified neural networks which satisfy norm properties and using the induced distance metric $N(x - y)$. They introduce two versions that we include as baselines: one (*Deepnorm*) parametrizes N with a modified ICNN that satisfies properties such as non-negativity and subadditivity. The second (*Widenorm*) computes a nonlinear transformation of a set of Mahalanobis norms. By construction, these metrics allow for asymmetry but still satisfy the triangle inequality. On the other hand, the Bregman divergence does not necessarily obey the triangle inequality. This is appealing for many situations, like image recognition where the triangle inequality may be too restrictive. As Pitis et al. [13] discuss, imposing the triangle inequality on other applications, such as language processing, is not obvious and needs further study.

We note that prior works are also computationally expensive, with *Deepnorm* requiring an $O(n^2)$ loop to compute pairwise distances, and *Deep-div* requiring a further $O(k)$ loop over max-affine components. In contrast, our approach can be vectorized as operations over tensors, resulting in the same computational complexity as the Euclidean distance. We discuss this further in Appendix E.

Information Retrieval and Bregman Divergences: As part of our goal in developing learnable Bregman divergences, we note that there is a long history of Bregman measures for information retrieval. Early work by Clayton showed that Bregman divergences have properties similar to the triangle inequality that allow for performing database searches in sub-linear time [20, 21]. Since then a number of works have explored improving nearest-neighbor retrieval speed under divergences so that more domain-specific asymmetric measures like KL-divergence or Itakura–Saito. This includes methods for accelerating exact neighbor retrieval [22–25] and faster approximate retrieval [26–28]. Our hope is that in future work these carefully chosen divergences may be instead learned from

Model	Exponential		Gaussian		Multinomial	
	Purity	Rand Index	Purity	Rand Index	Purity	Rand Index
Deep-div	0.665 <small>0.12</small>	0.788 <small>0.08</small>	0.867 <small>0.12</small>	0.910 <small>0.07</small>	0.876 <small>0.08</small>	0.919 <small>0.04</small>
Euclidean	0.365 <small>0.02</small>	0.615 <small>0.02</small>	0.782 <small>0.11</small>	0.869 <small>0.05</small>	0.846 <small>0.09</small>	0.900 <small>0.05</small>
Mahalanobis	0.452 <small>0.05</small>	0.697 <small>0.02</small>	0.908 <small>0.06</small>	0.935 <small>0.03</small>	0.894 <small>0.06</small>	0.926 <small>0.03</small>
NBD	0.735 <small>0.08</small>	0.830 <small>0.03</small>	0.913 <small>0.05</small>	0.938 <small>0.03</small>	0.921 <small>0.02</small>	0.939 <small>0.01</small>
PBDL	0.718 <small>0.08</small>	0.830 <small>0.04</small>	0.806 <small>0.14</small>	0.874 <small>0.09</small>	0.833 <small>0.08</small>	0.895 <small>0.04</small>

Table 1: We cluster data generated from a mixture of exponential, Gaussian, and multinomial distributions. Learning the metric from data is superior to using a standard metric such as Euclidean. Our approach NBD furthermore outperforms all other divergence learning methods. Means and standard deviations are reported over 10 runs.

the data, in the same manner that differentiable learning has improved image, speed, and signal classification in recent years.

4 Divergence learning experiments

We conduct several experiments that validate our approach as an effective means of learning divergences across a number of tasks. In the first section 4.1 we demonstrate that NBD *effectively learns standard Bregman retrieval and clustering benchmarks*, comparing favorably with the previous Bregman methods PBDL [7] and Deep-div [6]. In addition, we construct a Bregman regression task in section 4.2 where the labels are known divergences over raw feature vectors, so that the *only learning task is that of the divergence itself*. Finally in section §4.3 we investigate the ability of our method to *learn the ground truth divergence while simultaneously learning to extract a needed representation*, training a sub-network’s parameters θ and our divergence ϕ jointly. This is typified by the “BregMNIST” benchmark, which combines learning the MNIST digits with the only supervisory signal being the ground truth divergence between the digit values. Refer to the Appendix for detailed training protocols and data generation procedures.

4.1 Bregman ranking and clustering

Our first task expands the distributional clustering experiments in [4, 6]. The datasets consist of mixtures of $N = 1000$ points in \mathbb{R}^{10} from five clusters, where the multivariate distribution given cluster identity is non-isotropic Gaussian, exponential, or multinomial. Given a distance metric, a generalized k-means algorithm can be used to cluster the data points. While standard metrics, such as L2-distance and KL-divergence, may be ideal for specific forms of data (e.g. isotropic Gaussian and simplex data, respectively), our goal is to learn an appropriate metric directly from a separate labeled training set. In particular, because Bregman divergences are uniquely associated with each member of the exponential family [4], our method is especially suited for clustering data from a wide range of distributions which may not be known ahead of time. To learn the metric from data, we apply triplet mining, including all triplets with non-zero loss [1]. We use the same method to train all models except for the Euclidean baseline, which requires no training, and PBDL where we directly use the authors’ Python code.

As shown in Table 1, our method NBD gives improved clustering over all distributions compared to all baselines. In particular, standard k-means with Euclidean distance is clearly inadequate. While the Mahalanobis baseline shows significant improvement, it is only comparable to NBD in the Gaussian case, where a matrix can be learned to scale the clusters to be isotropic. This task indicates the importance of learning flexible divergences from data.

After demonstrating success in distributional clustering, we now apply our method to ranking and clustering real data (Table 2). For the ranking tasks, the test set is treated as queries for which the learned model retrieves items from the training set in order of increasing divergence. The ranking is scored using mean average precision (MAP) and area under ROC curve (AUC). Our method again outperforms the other Bregman learning methods in the large majority of datasets and metrics.

4.2 Divergence regression

As a confirmation that our method can faithfully represent Bregman divergences, we use simulated data to demonstrate that our method efficiently learns divergences between pairs of inputs. We generate pairs of 20-dim. vectors from a standard Normal distribution, with 10 informative features

Correlation	Euclidean			Mahalanobis			$x \log x$			KL		
	None	Med	High									
NBD	<i>0.17</i>	<i>0.15</i>	<i>0.16</i>	<i>0.16</i>	<i>0.18</i>	0.20	0.52	0.54	0.57	0.19	0.19	0.19
Deepnorm	3.56	3.97	4.15	7.70	5.97	7.66	1.59	1.74	1.79	0.30	0.28	0.28
Mahalanobis	0.00	0.03	0.05	0.02	0.04	0.09	<i>1.45</i>	1.67	1.72	0.23	0.22	0.22
Deep-div	7.78	7.81	7.84	17.92	12.26	14.15	2.59	2.67	2.70	0.44	0.50	0.51
Widenorm	3.56	3.99	4.12	7.73	6.01	7.60	1.49	<i>1.48</i>	<i>1.48</i>	0.30	0.28	0.28

Table 3: Regression test MAE when unused distractor features are correlated (None/Med/High) with the true/used features. Best results in **bold**, second best in *italics*.

used to compute the target divergence and 10 distractors. To be more challenging and realistic, we add various levels of correlations among all features to make the informative features harder to separate.

The following target divergences are used: 1) squared Euclidean distance (symmetric); 2) squared Mahalanobis distance (symmetric); 3) $\phi(x) = x \log x$ (asymmetric); 4) KL-divergence (asymmetric). In this task we compare our NBD with Deep-div and Mahalanobis, while the PBBL method does not scale to data of this size. Instead we add Deepnorm and Widenorm metrics from Pitis et al. [13] as alternative baselines which do not learn Bregman divergences.

The results of these experiments are in Fig. 1, with errors in Table 3. In the symmetric cases of the Euclidean and Mahalanobis ground-truth, our NBD method performs almost equivalently to learning a Mahalanobis distance itself. This shows that our method is not losing any representational capacity in being able to represent these standard measures. This is notably not true for the prior approaches for asymmetric learning: Deepnorm, Widenorm, and Deep-div. Notably, unlike in the clustering tasks, Deep-div is unable to accurately represent even the most common Bregman regression targets, due to its piecewise representation of ϕ . In Fig. 1c and Fig. 1d two asymmetric divergences are used, and our NBD approach performs better than all existing options. Because these experiments isolate purely the issue of learning the divergence itself, we have strong evidence that our approach is the most faithful to learning a known divergence from a supervisory signal. Note that the Mahalanobis distance performed second best under all noise levels, meaning the prior asymmetric methods were less accurate at learning asymmetric measures than choosing a purely symmetric parameterization.

Dataset	Model	MAP	AUC	Purity	Rand Index
abalone	Deep-div	0.281	0.645	0.377	0.660
	Euclidean	0.301	0.666	0.422	0.750
	Mahalanobis	0.310	0.677	0.419	0.750
	NBD	0.316	0.682	0.432	0.750
	PBBL	0.307	0.659	0.386	0.735
balance scale	Deep-div	0.804	0.859	0.869	0.828
	Euclidean	0.611	0.666	0.633	0.568
	Mahalanobis	0.822	0.854	0.851	0.761
	NBD	0.887	0.915	0.898	0.872
	PBBL	0.836	0.855	0.872	0.814
car	Deep-div	0.787	0.757	0.852	0.750
	Euclidean	0.681	0.589	0.704	0.523
	Mahalanobis	0.787	0.752	0.778	0.654
	NBD	0.820	0.803	0.860	0.758
	PBBL	0.798	0.775	0.854	0.750
iris	Deep-div	0.945	0.967	0.811	0.820
	Euclidean	0.827	0.897	0.820	0.828
	Mahalanobis	0.946	0.973	0.884	0.879
	NBD	0.957	0.977	0.909	0.902
	PBBL	0.943	0.967	0.889	0.888
transfusion	Deep-div	0.648	0.525	0.756	0.621
	Euclidean	0.666	0.536	0.748	0.563
	Mahalanobis	0.680	0.570	0.750	0.543
	NBD	0.695	0.603	0.756	0.600
	PBBL	0.637	0.504	0.748	0.622
wine	Deep-div	0.983	0.987	0.953	0.947
	Euclidean	0.844	0.884	0.902	0.887
	Mahalanobis	0.949	0.970	0.944	0.940
	NBD	0.969	0.980	0.960	0.948
	PBBL	0.978	0.982	0.820	0.823

Table 2: Across several real datasets, a learned Bregman divergence is superior to Euclidean or Mahalanobis metrics for downstream ranking (MAP, AUC) and clustering (Purity, Rand Index) tasks. Our approach NBD consistently outperforms prior Bregman learning approaches, Deep-div and PBBL, on most datasets. See Appendix Table 8 for standard deviation results.

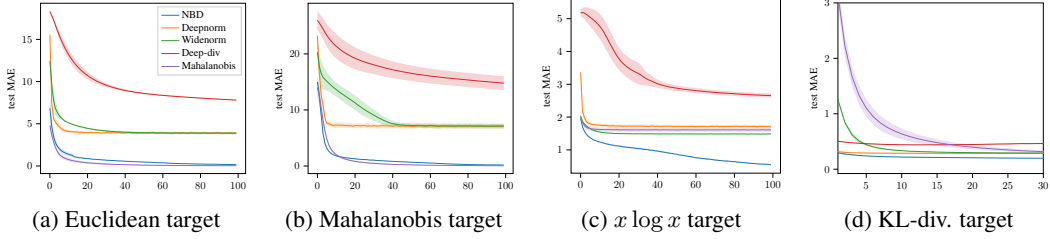


Figure 1: Results when vectors with 10 real features and 10 distractor features are used to compute different specific Bregman divergences. Mean absolute error is on the y-axis and number of training epochs on the x-axis. The shaded region around each plot shows the standard deviation of the results. Note in all cases our NBD has very low variance while effectively learning the target divergence.

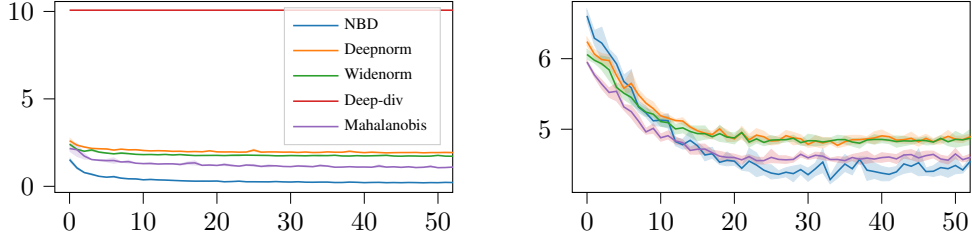


Figure 3: MSE (y-axis) after epochs of training (x-axis) on asymmetric BregMNIST (left) and BregCIFAR (right). NBD performs best in both tasks. Symmetric case in Appendix.

4.3 Co-learning an embedding with a divergence

Finally, we introduce a prototype task, BregMNIST, where a neural embedding must be learned along with the divergence metric. The dataset consists of paired MNIST images, with the target distance being a Bregman divergence between the digits shown in the images. Example pairs are displayed in Fig. 2 for the asymmetrical Bregman divergence parametrized by $\phi(x) = (x + 1) \log(x + 1)$.

We additionally make a harder version by substituting MNIST with CIFAR10 with the same divergence labels. In both cases the relation of features to class label is arbitrary (that is, we impose an ordinal relation among labels that does not exist in the data), meaning that the embedding function effectively maps image classes to the correct number used to compute the divergence. The results of the experiments (Fig. 3) mirror our results in §4.2. For both BregMNIST and BregCIFAR NBD performs best, while prior methods of learning asymmetric measures perform worse than the Mahalanobis distance.

5 Non-Bregman Learning

We have shown that our NBD method is the most effective among all available options when the underlying ground-truth is from the class of Bregman divergences. In this section we will now explore the effectiveness of our approach on tasks that are known to be non-Euclidean, but not necessarily representable by a Bregman divergence. The purpose of these experiments is to show that NBD does not depend on the underlying representation being a proper divergence in order to still be reasonably effective, and that it is still more effective than the prior Deep-div approach to Bregman learning. This is also of practical relevance to applications: just as the Euclidean metric was used for convenient properties and simplicity, without belief that the underlying system was truly Euclidean, our NBD may be valuable for developing more flexible methods that inherit the mathematical convenience of Bregman divergences.

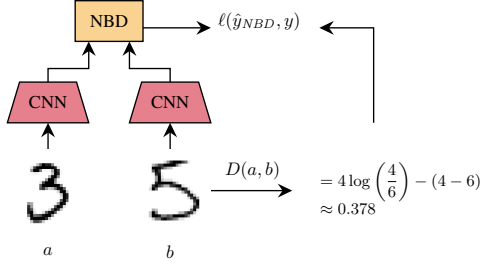


Figure 2: Demonstration of the BregMNIST task. Nodes with the same color indicate weight sharing. Each image is embedded by a CNN, and the ground-truth divergence is computed from the digit values of the input images. The embeddings of each image are given to NBD, and the loss is computed from NBD’s output and the true divergence. The CNN and NBD are learned jointly.

When the underlying ground-truth is from the class of Bregman divergences. In this section we will now explore the effectiveness of our approach on tasks that are known to be non-Euclidean, but not necessarily representable by a Bregman divergence. The purpose of these experiments is to show that NBD does not depend on the underlying representation being a proper divergence in order to still be reasonably effective, and that it is still more effective than the prior Deep-div approach to Bregman learning. This is also of practical relevance to applications: just as the Euclidean metric was used for convenient properties and simplicity, without belief that the underlying system was truly Euclidean, our NBD may be valuable for developing more flexible methods that inherit the mathematical convenience of Bregman divergences.

These tasks probe the efficacy of the closest Bregman approximation of the underlying divergence. We therefore expect that our method will not surpass the state-of-the-art when the task is sufficiently non-Bregman.

5.1 Approximate Semantic Distance

The first task evaluates learning symmetric distances that do not follow the triangle inequality. We group the CIFAR10 classes into two categories: man-made and natural. Within each category we select an arbitrary exemplar class (*car* and *deer* in our experiment). We then assign proxy distances between classes to reflect semantic similarity: 0.5 within the same class, 2 between any non-exemplar class and its category exemplar, and 8 between non-exemplar classes within a category. Pairs from different categories are not compared. Besides disobeying the triangle inequality, the distance values do not reflect any known divergence, and can be changed arbitrarily.

Like BregCIFAR, we present pairs of images to the model, which simultaneously adjusts a neural embedding and learn a divergence function such that inter-class distances in the embedding space match the target values. This task is harder than the previous ones because it is not sufficient to learn a separable embedding for each class; the embeddings must additionally be arranged appropriately in a non-Euclidean space. The results in Table 4 indicate our method effectively learns distances that do not follow the triangle inequality. Interestingly the Deep-div approach does second-best here due to the small space of valid outputs. The other approaches by limitation adhere to the triangle inequality and do not perform as well.

5.2 Overlap distance

The overlap distance task presents pairs of the same image or different images, but with different crops taken out. A horizontal and vertical cut are chosen uniformly at random from each image. When the crops are based on the same image, the asymmetrical divergence measure between images X and Y is the percent intersection area: $D(X, Y) = 1 - \frac{|X \cap Y|}{|X|}$. Otherwise the divergence is 1. We use the INRIA Holidays dataset (see Appendix D). The results can be found in Fig. 4, where we see NBD performs the second best of all options.

We observe that Widenorm performs better on this task, especially during the initial learning process, due to the fact that it is permitted to violate the positive definiteness property of norms: $D(x, x) > 0$. Thus the method learns to map a difference of zero between embeddings to some intermediate distance with lower MSE. This can be problematic in use cases where the definiteness is an important property.

5.3 Shortest path length

Our final task is one that inherently favors the Widenorm and Deepnorm methods because they maintain the triangle inequality (i.e., no shortcuts allowed in shortest path), and so are expected to perform better than NBD. They are included so that we may further compare our NBD with the Deep-div approach, the only other method for learning deep Bregman divergences. We reproduce the experimental setup of Pitis et al. [13] closely with details in Appendix C.

The results for each method are shown in Table 5, which largely match our expectations. The triangle-inequality preserving measures usually perform best, which makes sense given the nature of the problem: any violation of the triangle inequality means the distance measure is “taking a shortcut” through the graph search space, and thus must be under-estimating the true distance to the target node. NBD and Deep-div, by being restricted to the space of Bregman divergences, have no constraint that prevents violating the triangle-inequality, and thus often under-estimate the true distances. We note that on the 3d dataset the NBD test performance is better than both deepnorm and widenorm, and is within 4% of the widenorm method on the octagon dataset. These results show that NBD is the most

Metric	Same	Unseen
NBD	0.04	3.52
Deepnorm	1.23	4.18
Mahalanobis	2.00	4.56
Deep-div	0.10	4.13
Widenorm	1.39	4.50

Table 4: MSE for CIFAR10 category semantic distance after 200 epochs. Our NBD performs the best on learned and previously unseen images.

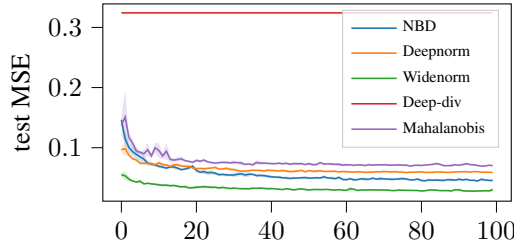


Figure 4: MSE (y-axis) for predicting the overlap between two image embeddings learned jointly with the underlying CNN.

Method	3d		3dd		octagon		taxi		traffic	
	Train	Test	Train	Test	Train	Test	Train	Test	Train	Test
NBD	4.34	33.49	19.91	337.59	4.67	25.32	3.11	66.27	2.53	12.03
Deepnorm	4.97	22.44	34.40	275.99	4.81	15.19	1.52	20.31	1.76	5.27
Mahalanobis	4.45	30.90	24.99	267.18	6.82	44.30	1.31	18.32	1.47	5.60
Deep-div	695.97	930.57	589.13	806.14	879.94	1046.08	489.80	625.16	399.14	618.94
Widenorm	4.49	27.92	25.76	253.65	5.17	23.46	1.18	16.20	1.44	5.21
Bregman-sqrt	5.94	27.59	27.70	266.25	8.62	40.18	1.57	19.02	1.63	5.23
Bregman-GS	4.50	30.51	23.78	266.91	7.26	43.13	1.17	16.71	1.55	5.49

Table 5: Results of learning measures on the shortest-path task. Triangle-inequality preserving deep and wide-norm are expected to perform best. Our NBD performs significantly better than previous Bregman learning approach Deep-div, and can be competitive with the triangle-inequality preserving methods. The gap between train and test loss shows the impact of triangle inequality helping to avoid over-fitting the observed sub-graph used for training.

viable option for learning a useful Bregman divergence, and performs considerably better than the prior Deep-div approach.

We include both the train and test losses in Table 5, as they allow us to further confirm the impact that triangle inequality property provides in avoiding overfitting the training sub-graph. The start/end pairs used in training do not need to worry about the triangle inequality because any over/under prediction is intrinsically corrected by the loss calculation and gradient update. Thus the training loss, for this task, demonstrates primarily the ability of each method to learn the asymmetric relationships. In 3/5 cases the Mahalanobis method has the lowest training error, but then increases more significantly on the test set — but not to an outrageous degree. This suggests that while the shortest paths problem from Pitis et al. [13] does stress the ability to correctly leverage the triangle inequality to avoid overfitting, it is not an ideal benchmark for general asymmetric learning.

We conduct further analysis to explore the degree to which the properties underlying Bregman divergences affect shortest path length learning. We introduce two extensions to NBD. The first is a soft modification encouraging the triangle inequality to be obeyed (Bregman-sqrt). The second has a hard constraint guaranteeing the triangle inequality (Bregman-GS). Results are in Table 5.

For the first we draw from mathematical literature demonstrating that metrics can be induced from the square root of certain symmetrized Bregman divergences, depending on constraints on ϕ [29]. We learn the square root of the Bregman divergence to provide a soft inductive bias (as an illustrative example, Euclidean distance is a metric but squared Euclidean distance is not).

For the second we introduce a modification of the Bregman divergence known as the Generalized Symmetrized Bregman divergence. As shown by Acharya et al. [30], the square root of such a divergence is guaranteed to satisfy the triangle inequality. This divergence is defined as $D_\phi^{gsb}(x, y) = D_\phi(x, y) + D_\phi(y, x) + \frac{1}{2}\|x - y\|_2^2 + \frac{1}{2}\|\nabla\phi(x) - \nabla\phi(y)\|_2^2$. There is an inherent tradeoff between the two extensions as Bregman-sqrt can be asymmetric but still does not require satisfying the triangle inequality, while Bregman-GS is symmetric but always satisfies the triangle inequality. We see that these two modifications to NBD are highly competitive with Deepnorm and Widenorm. Furthermore, the relative performance of each provides an indication of whether asymmetry or triangle inequality is more crucial to modeling a given dataset. These methods highlight that even when a given task is highly non-Bregman, NBD can be readily extended to relax or strengthen various assumptions to better model the data.

6 Conclusion

To enable future asymmetric modeling research, we have developed the Neural Bregman Divergence (NBD). NBD jointly learns a Bregman measure and a feature extracting neural network. We show that NBD learns divergences directly or indirectly when trained jointly with a network, and that NBD still learns effectively when the underlying metric is not a divergence, allowing effective use of our tool across a wide spectrum but retaining the nice properties of Bregman divergences.

References

- [1] E. Hoffer and N. Ailon, “Deep metric learning using triplet network,” in *International workshop on similarity-based pattern recognition*. Springer, 2015, pp. 84–92.
- [2] C. Huang, C. C. Loy, and X. Tang, “Local similarity-aware deep feature embedding,” in *NeurIPS*, 2016.
- [3] D. Zhang, Y. Li, and Z. Zhang, “Deep metric learning with spherical embedding,” in *NeurIPS*, 2020.
- [4] A. Banerjee, S. Merugu, I. S. Dhillon, J. Ghosh, and J. Lafferty, “Clustering with bregman divergences.” *Journal of machine learning research*, vol. 6, no. 10, 2005.
- [5] L. Bregman, “The relaxation method of finding the common point of convex sets and its application to the solution of problems in convex programming,” *USSR Computational Mathematics and Mathematical Physics*, vol. 7, no. 3, pp. 200–217, jan 1967.
- [6] H. K. Cilingir, R. Manzelli, and B. Kulis, “Deep divergence learning,” in *ICML*, 2020.
- [7] A. Siahkamari, X. Xia, V. Saligrama, D. Castañón, and B. Kulis, “Learning to approximate a bregman divergence,” in *NeurIPS*, vol. 33, 2020, pp. 3603–3612.
- [8] H. Drucker and Y. Le Cun, “Double backpropagation increasing generalization performance,” in *IJCNN*. IEEE, 1991, pp. 145–150.
- [9] R. Frostig, M. Johnson, D. Maclaurin, A. Paszke, and A. Radul, “Decomposing reverse-mode automatic differentiation,” in *POPL*, 2021.
- [10] A. Paszke, S. Gross, S. Chintala, G. Chanan, E. Yang, Z. DeVito, Z. Lin, A. Desmaison, L. Antiga, and A. Lerer, “Automatic differentiation in pytorch,” 2017.
- [11] B. Amos, L. Xu, and J. Z. Kolter, “Input convex neural networks,” in *ICML*, 2017.
- [12] Y. Chen, Y. Shi, and B. Zhang, “Optimal control via neural networks: A convex approach,” in *ICLR*, 2019.
- [13] S. Pitis, H. Chan, K. Jamali, and J. Ba, “An inductive bias for distances: Neural nets that respect the triangle inequality,” *arXiv preprint arXiv:2002.05825*, 2020.
- [14] P. Jain, B. Kulis, J. V. Davis, and I. S. Dhillon, “Metric and kernel learning using a linear transformation,” *The Journal of Machine Learning Research*, vol. 13, pp. 519–547, 2012.
- [15] B. Kulis *et al.*, “Metric learning: A survey,” *Foundations and trends in machine learning*, vol. 5, no. 4, pp. 287–364, 2012.
- [16] K. Musgrave, S. Belongie, and S.-N. Lim, “A metric learning reality check,” in *ECCV*, 2020.
- [17] E. P. Xing, A. Y. Ng, M. I. Jordan, and S. Russell, “Distance metric learning with application to clustering with side-information,” in *NeurIPS*, vol. 15, no. 505–512. Citeseer, 2002, p. 12.
- [18] B. Kulis, M. A. Sustik, and I. S. Dhillon, “Low-rank kernel learning with bregman matrix divergences.” *Journal of Machine Learning Research*, vol. 10, no. 2, 2009.
- [19] L. Wu, R. Jin, S. C. Hoi, J. Zhu, and N. Yu, “Learning bregman distance functions and its application for semi-supervised clustering,” in *NeurIPS*, 2009.
- [20] L. Cayton, “Fast Nearest Neighbor Retrieval for Bregman Divergences,” in *ICML*. New York, NY, USA: ACM, 2008, pp. 112–119.
- [21] ——, “Efficient Bregman Range Search,” in *NeurIPS*. USA: Curran Associates Inc., 2009, pp. 243–251.
- [22] F. Nielsen, P. Piro, and M. Barlaud, “Bregman vantage point trees for efficient nearest Neighbor Queries,” in *2009 IEEE International Conference on Multimedia and Expo*. IEEE, jun 2009, pp. 878–881.

- [23] Y. Song, Y. Gu, R. Zhang, and G. Yu, “BrePartition: Optimized High-Dimensional kNN Search with Bregman Distances,” *IEEE Transactions on Knowledge and Data Engineering*, pp. 1–1, 2020.
- [24] A. Abdullah and S. Venkatasubramanian, “A Directed Isoperimetric Inequality with Application to Bregman Near Neighbor Lower Bounds,” in *ACM Symposium on Theory of Computing*. New York, NY, USA: Association for Computing Machinery, 2015, pp. 509–518.
- [25] Z. Zhang, B. C. Ooi, S. Parthasarathy, and A. K. H. Tung, “Similarity Search on Bregman Divergence: Towards Non-metric Indexing,” in *VLDB*, 2009, pp. 13–24.
- [26] A. Abdullah, J. Moeller, and S. Venkatasubramanian, “Approximate Bregman near Neighbors in Sublinear Time: Beyond the Triangle Inequality,” in *Annual Symposium on Computational Geometry*, ser. SoCG ’12, New York, NY, USA, 2012, pp. 31–40.
- [27] B. Naidan and M. L. Hetland, “Bregman Hyperplane Trees for Fast Approximate Nearest Neighbor Search,” *International Journal of Multimedia Data Engineering and Management*, vol. 3, no. 4, pp. 75–87, oct 2012.
- [28] Y. Mu and S. Yan, “Non-Metric Locality-Sensitive Hashing,” in *AAAI*, 2010.
- [29] P. Chen, Y. Chen, M. Rao *et al.*, “Metrics defined by bregman divergences,” *Communications in Mathematical Sciences*, vol. 6, no. 4, pp. 915–926, 2008.
- [30] S. Acharyya, A. Banerjee, and D. Boley, “Bregman divergences and triangle inequality,” in *ICDM*, 2013, pp. 476–484.
- [31] K. He, X. Zhang, S. Ren, and J. Sun, “Deep residual learning for image recognition,” in *Proceedings of the IEEE conference on computer vision and pattern recognition*, 2016, pp. 770–778.
- [32] H. Jegou, D. Mattheijns, and C. Schmid, “Hamming embedding and weak geometry consistency for large scale image search–extended version–,” 2008.
- [33] B. Charlier, J. Feydy, J. A. Glaunès, F.-D. Collin, and G. Durif, “Kernel operations on the gpu, with autodiff, without memory overflows,” *Journal of Machine Learning Research*, vol. 22, no. 74, pp. 1–6, 2021.

A Data generation details

Distributional clustering. We sample 1000 points uniformly into 5 clusters, each with 10 feature dimensions. To generate non-isotropic Gaussians we sample means uniformly in the hyper-box within $[-4, 4]$ for each coordinate. The variances are a random PSD matrix (scikit-learn `make_spd_matrix`) added with $\sigma^2 I$ where $\sigma^2 = 5$. The reason for these values are because we aimed to have each mixture task be similarly difficult (clusters not perfectly separable but also not too challenging). For the multinomial task, we sampled 100 counts into the 10 feature dimensions. Each cluster’s underlying probability distribution was sampled from $Dirichlet([10, 10, \dots, 10])$. Finally, the exponential case are iid samples for each feature. The underlying cluster rates are sampled uniformly between [0.1, 10].

Regression noise features. To add correlation among features (both informative and distractors), we generate covariance matrices with controlled condition number κ while keeping the marginal distributions of each feature as $x_i \sim \mathcal{N}(0, 1)$. For the medium correlation task $\kappa < 100$, while for high correlation κ is between 250 and 500.

50000 pairs were generated with 20 features.

B Experimental procedure

In all metric learning tasks, we fit all models using triplet mining, with margin 0.2, and Adam optimizer.

Distributional clustering. We used batch size 128, 200 epochs, 1e-3 learning rate for all models. Here, and in all subsequent experiments, to train PBDL we used the authors’ provided Python code, which uses the alternating direction method of multipliers (ADMM) technique. (They also provide Matlab code using Gurobi.)

Bregman ranking. Since Deep-div and NBD are deep learning approaches, we use Adam to optimize this problem instead of convex optimization solvers. To ensure convergence, we tune the learning rate and number of epochs using gridsearch over a validation set separated from the training data. We do the same for the Mahalanobis approach. A typical example of the parameters is batch size 256, 250 epochs, learning rate 1e-3.

Regression. We used 100 epochs of training with learning rate 1e-3, batch size 1000.

Deep learning experiments. For the remaining experiments which involve co-learning an embedding, we use default hyperparameter settings to keep methods comparable, such as Adam optimizer, learning rate 1e-3, batch size 128, embedding dimension 128, and 200 epochs.

For the MNIST/CIFAR tasks the embedding network consists of two/four convolutional layers respectively followed by two fully-connected layers (more specific details follow). For the semantic distance CIFAR task, we used a pretrained ResNet20 as the embedding without freezing any layers for faster learning [31]. Results were robust to the embedding model chosen.

We replicated each training and reported means and standard deviations. For the Bregman benchmark tasks we trained 20x, while for the deep learning/graph learning tasks we trained 5x. Learning curves in the figures show mean and 95% confidence interval for the loss over each epoch. We used Quadro RTX 6000 GPUs to train our models.

C Shortest Path Details

Pitis et al. [13] introduced learning shortest path length in graphs as a task. The problem consists of learning $d(x, y)$ where $x, y \in \mathcal{V}$ are a pair of nodes in a large weighted graph $G = (\mathcal{V}, \mathcal{E})$. For each node, the predictive features consist of shortest distances from the node to a set of 32 landmark nodes (and vice versa for asymmetric graphs). As this task requires predicting the distance from one node to another, maintaining the triangle inequality has inherent advantages and is the correct inductive bias for the task. We still find the task useful to elucidate the difference between NBD and the prior Deep-div.

We reproduce the experimental setup of Pitis et al. [13] closely, collecting a 150K random subset of pairs from the graph as the dataset, with true distances computed using A^* search. While the original work normalized distances to mean 50, we found that such large regression outputs were difficult to learn. Instead we normalize to mean 1, which results in faster convergence of all methods. A

Dataset	Asymmetric	Dimension	Edge weights	Details
3d taxi	No	50x50x50 cubic grid	uniform $\{0.01, 0.02, \dots, 1.00\}$	edges wrap around
	No	25x25x25x25 (two objects on 2d grid)	uniform $\{0.01, 0.02, \dots, 1.00\}$	no wrap
3dd traffic	Yes	50x50x50 cubic grid	uniform $\{0.01, 0.02, \dots, 1.00\}$	only one edge in each dimension is available
	Yes	100x100 2d grid	forward and reverse sampled from Normal with mean from uniform $\{0.01, 0.02, \dots, 1.00\}$	no wrap
octagon	Yes	100x100 2d grid, diagonals connected	forward and reverse sampled from Normal with mean from uniform $\{0.01, 0.02, \dots, 1.00\}$	no wrap

Table 6: Details of the shortest-path datasets, the number of dimensions in the graph, and how the edge weights in the graph are computed. These tasks were originally proposed by [13] and favor asymmetric methods that maintain the triangle inequality.

50K/10K train-test split was used. The features are standardized with added noise sampled from $\mathcal{N}(0, 0.2)$, and 96 normal-distributed distractor features were included. For additional details refer to Appendix E of [13]. However, their experimental detail and code was sufficient to only reproduce three of the graph datasets (3d, taxi, 3dd). Therefore, we develop two additional asymmetric graphs (traffic and octagon). The details of all the shortest-path graphs we use are provided in Table 6. Models were trained for 50 epochs at learning rate 5e-5 and 50 epochs at 5e-6.

C.1 Additional hyperparameter details

We followed the hyperparameter specifications for the Deepnorm and Widenorm results as stated in [13]. The Widenorm used 32 components with size 32, concave activation size 5, and max-average reduction. For the Deepnorm we used the neural metric version which gave the strongest performance in their paper: 3 layers with dimension 128, MaxReLU pairwise activations, concave activation size 5, and max-average reduction. We adapt their PyTorch code from <https://github.com/spitis/deepnorms>. In the graph distance task, results show the same learning pattern (and relative performances between models) but the overall error magnitudes that we obtain are rather different than their reported results.

We re-implemented the Deep-div method following the description in [6]. The number of affine sub-networks stated in their paper varied but was generally set to low values such as 10, for the purpose of matching the number of classes in their classification tasks. In their appendix they experiment with increasing numbers of sub-networks and find best results at 50. For this reason we set 50 for our experiments. Following their paper, we use FNNs for the max-affine components.

Our NBD uses a 2 hidden layer FICNN with width 128 for ϕ .

D Overlap Details

We use the INRIA Holidays dataset [32], which contains over 800 high-quality vacation pictures contributed by the original authors. Many consecutive-numbered images (e.g. 129800.jpg, 129801.jpg, 129802.jpg) are retakes of the same scene, which would interfere with assigning zero overlap to different images. To address this we only use images ending in 00.jpg, which are all different scenes. This leaves 300 images, which we resize to 72x72 then apply a 64x64 center-crop. The training set consists of 10,000 pairs sampled with random crops each epoch from the first 200 of the images, while the test set is a fixed set of 10,000 pairs with crops drawn from the last 100. We set a 25% chance for a given pair to come from different images and receive a divergence of 1. All models were trained with batch size 128, Adam optimizer with learning rate 5e-4, and embedding dimension of 128. The embedding network consists of four 3x3 convolutional layers (32, 64, 128, 256 filters respectively) with 2x2 max pooling layers followed by two linear layers with hidden dimension 256.

We compute overlap as the percent of non-intersecting area from the crops. We show this in Fig. 5.

E Computational discussion

We measure timing information of NBD as well as the benchmarks used in our experiments for a divergence learning task as in §4.2. The training time (forward and backward passes), inference time (forward pass), and pairwise distance matrix computation are collected. While the pairwise distance is not directly used in our experiments, it is commonly computed in metric learning applications such as clustering and classification. The data dimension size $N \times D$ used here is characteristic of the size

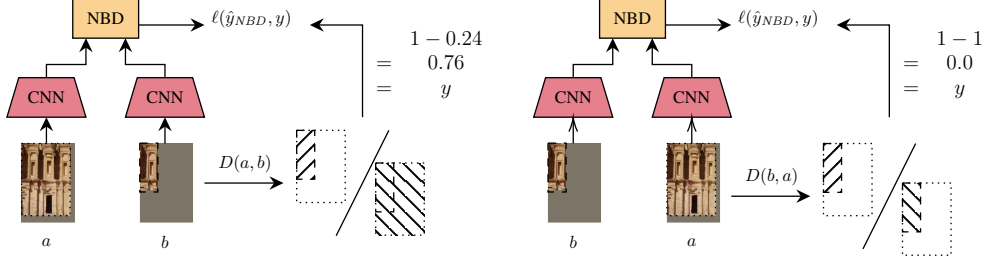


Figure 5: Demonstration of how the overlap distance is computed in our setup. Ground-truth distance is the intersection of the shared images divided by the area of the first image.

of many metric learning experiments, where the $N \times N$ pairwise distance matrix can be stored on GPU memory, but the $N \times N \times D$ tensor with embedding dimension D does not fit: the fast but naive approach of flattening the matrix and passing as a $N \times N$ -length batch does not work.

The Mahalanobis method is naturally the fastest method and serves as a reasonable runtime lower bound. This is because the distance can be expressed a simple composition of a norm with a linear layer. The squared Euclidean norm can be simplified as $D(x, y) = \|x\|_2^2 + \|y\|_2^2 - 2\langle x, y \rangle$, which can be efficiently computed. We can similarly compute the Bregman divergences. For example, the squared Euclidean distance is equivalently written as $D(x, y) = \|x\|_2^2 - \|y\|_2^2 - \langle 2y, x - y \rangle$, which is its Bregman divergence formulation. Though not necessary for our current experiments, the pairwise distances for larger batch sizes for the Mahalanobis and NBD can be readily implemented in PyKeOps [33]. Thus the longer computational time for NBD can likely be attributed to the increased cost of double backpropagation and the convex metric architecture.

Table 7: Timing information for a divergence learning task as in §4.2, with embedding dimension 20 and a batch size of 1000, comparing the methods used in our experiments. We compute the per-epoch training time (forward and backward passes), inference time (forward pass), and pairwise distance matrix computation. Results are averaged over 30 runs, with standard deviation in parentheses.

Method	Training	Inference	Pairwise distance
NBD	0.73 (0.08)	0.10 (0.03)	0.52 (0.06)
Deep-div	1.63 (0.11)	0.12 (0.02)	0.59 (0.03)
Deepnorm	0.81 (0.07)	0.09 (0.02)	4.53 (0.03)
Widenorm	0.52 (0.04)	0.08 (0.02)	2.61 (0.03)
Mahalanobis	0.46 (0.03)	0.08 (0.02)	0.40 (0.03)

On the other hand, the Deepnorm cannot be vectorized in such manner, so pairwise distances need to be computed on the order of $O(N^2)$ runtime, for example by further splitting the tensor into smaller mini-batches. While the Widenorm is composed of Mahalanobis metrics (set to 32 in our experiments) that can be vectorized, in our experiments the memory requirement was still too high, also requiring looping over sub-batches. We use sub-batch size 200 in this analysis. We note that the loop can be alternatively performed over the Mahalanobis components in Widenorm, but this would still be slower than the standard Mahalanobis and NBD methods. Finally, the Deep-div method efficiently computes pairwise distances, but its forward pass requires the input to be passed through a set of affine sub-networks, increasing the computational time.

F Bregman ranking and clustering standard deviations

Full version of Table 2. Standard deviations in small font, means in regular font.

Dataset	Model	MAP	AUC	Purity	Rand Index
abalone	Deep-div	0.281 <small>0.01</small>	0.645 <small>0.02</small>	0.377 <small>0.02</small>	0.660 <small>0.04</small>
	Euclidean	0.301 <small>0.01</small>	0.666 <small>0.01</small>	0.422 <small>0.03</small>	0.750 <small>0.01</small>
	Mahalanobis	0.310 <small>0.01</small>	0.677 <small>0.01</small>	0.419 <small>0.02</small>	0.750 <small>0.01</small>
	NBD	0.316 <small>0.01</small>	0.682 <small>0.01</small>	0.432 <small>0.03</small>	0.750 <small>0.01</small>
	PBDL	0.307 <small>0.01</small>	0.659 <small>0.01</small>	0.386 <small>0.02</small>	0.735 <small>0.02</small>
balance-scale	Deep-div	0.804 <small>0.03</small>	0.859 <small>0.02</small>	0.869 <small>0.02</small>	0.828 <small>0.03</small>
	Euclidean	0.611 <small>0.01</small>	0.666 <small>0.01</small>	0.633 <small>0.06</small>	0.568 <small>0.04</small>
	Mahalanobis	0.822 <small>0.01</small>	0.854 <small>0.01</small>	0.851 <small>0.06</small>	0.761 <small>0.05</small>
	NBD	0.887 <small>0.01</small>	0.915 <small>0.01</small>	0.898 <small>0.02</small>	0.872 <small>0.03</small>
	PBDL	0.836 <small>0.02</small>	0.855 <small>0.02</small>	0.872 <small>0.02</small>	0.814 <small>0.03</small>
car	Deep-div	0.787 <small>0.01</small>	0.757 <small>0.01</small>	0.852 <small>0.04</small>	0.750 <small>0.04</small>
	Euclidean	0.681 <small>0.00</small>	0.589 <small>0.00</small>	0.704 <small>0.02</small>	0.523 <small>0.03</small>
	Mahalanobis	0.787 <small>0.01</small>	0.752 <small>0.01</small>	0.778 <small>0.02</small>	0.654 <small>0.03</small>
	NBD	0.820 <small>0.01</small>	0.803 <small>0.01</small>	0.860 <small>0.01</small>	0.758 <small>0.02</small>
	PBDL	0.798 <small>0.01</small>	0.775 <small>0.01</small>	0.854 <small>0.01</small>	0.750 <small>0.02</small>
iris	Deep-div	0.945 <small>0.03</small>	0.967 <small>0.02</small>	0.811 <small>0.16</small>	0.820 <small>0.16</small>
	Euclidean	0.827 <small>0.02</small>	0.897 <small>0.01</small>	0.820 <small>0.07</small>	0.828 <small>0.05</small>
	Mahalanobis	0.946 <small>0.03</small>	0.973 <small>0.01</small>	0.884 <small>0.12</small>	0.879 <small>0.11</small>
	NBD	0.957 <small>0.02</small>	0.977 <small>0.01</small>	0.909 <small>0.10</small>	0.902 <small>0.10</small>
	PBDL	0.943 <small>0.03</small>	0.967 <small>0.02</small>	0.889 <small>0.14</small>	0.888 <small>0.13</small>
transfusion	Deep-div	0.648 <small>0.01</small>	0.525 <small>0.02</small>	0.756 <small>0.03</small>	0.621 <small>0.04</small>
	Euclidean	0.666 <small>0.01</small>	0.536 <small>0.01</small>	0.748 <small>0.03</small>	0.563 <small>0.04</small>
	Mahalanobis	0.680 <small>0.01</small>	0.570 <small>0.01</small>	0.750 <small>0.03</small>	0.543 <small>0.05</small>
	NBD	0.695 <small>0.01</small>	0.603 <small>0.01</small>	0.756 <small>0.03</small>	0.600 <small>0.04</small>
	PBDL	0.637 <small>0.01</small>	0.504 <small>0.01</small>	0.748 <small>0.03</small>	0.622 <small>0.03</small>
wine	Deep-div	0.983 <small>0.02</small>	0.987 <small>0.01</small>	0.953 <small>0.08</small>	0.947 <small>0.08</small>
	Euclidean	0.844 <small>0.02</small>	0.884 <small>0.02</small>	0.902 <small>0.07</small>	0.887 <small>0.06</small>
	Mahalanobis	0.949 <small>0.02</small>	0.970 <small>0.01</small>	0.944 <small>0.10</small>	0.940 <small>0.09</small>
	NBD	0.969 <small>0.02</small>	0.980 <small>0.01</small>	0.960 <small>0.05</small>	0.948 <small>0.06</small>
	PBDL	0.978 <small>0.02</small>	0.982 <small>0.01</small>	0.820 <small>0.14</small>	0.823 <small>0.12</small>

Table 8: Across several real datasets, a learned Bregman divergence is superior to Euclidean or Mahalanobis metrics for downstream ranking (MAP, AUC) and clustering (Purity, Rand Index) tasks. Furthermore, our approach NBD consistently outperforms the prior Bregman learning approaches, Deep-div and PBDL, on most datasets. MAP = mean average precision, AUC = area under curve

G Enlarged Figure

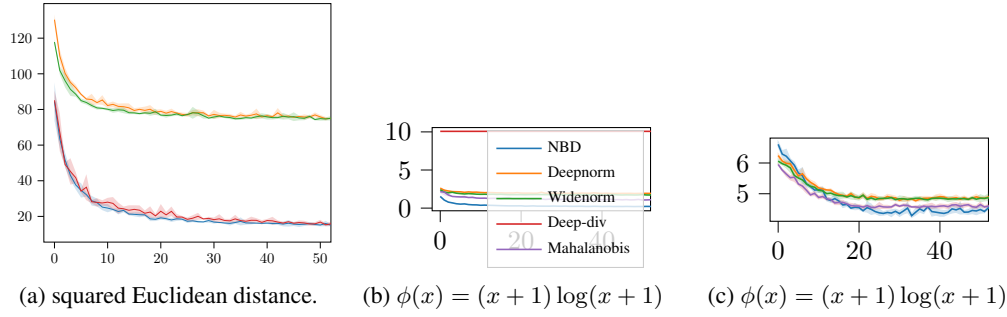


Figure 6: MSE (y-axis) after epochs of training (x-axis), where NBD performs best in the symmetric (left) and asymmetric (center, right) Bregman learning tasks. The first two tasks are BregMNIST and the third is BregCIFAR. The same legend applies to all figures.